Preprints.org

Article

Not peer-reviewed version

Analysis of Adaptive Algorithms Based on Least-Mean-Square Applied to Hand Tremors Suppression Control

Rafael Silfarney Alves Araújo , Jessica Cristina Tironi , Wemerson Delcio Parreira * , Renata Coelho Borges , Juan Francisco De Paz Santana * , Valderi Reis Quietinho Leithardt *

Posted Date: 6 February 2023

doi: 10.20944/preprints202302.0092.v1

Keywords: Adaptive Algorithm; Tremor Suppression; LMS; Parkinson

Preprints.org is a free multidiscipline platform providing preprint service that is dedicated to making early versions of research outputs permanently available and citable. Preprints posted at Preprints.org appear in Web of Science, Crossref, Google Scholar, Scilit, Europe PMC.

Copyright: This is an open access article distributed under the Creative Commons Attribution License which permits unrestricted use, distribution, and reproduction in any medium, provided the original work is properly cited.

Preprints (www.preprints.org) | NOT PEER-REVIEWED | Posted: 6 February 2023 doi:10.20944/preprints202302.0092.v1

Disclaimer/Publisher's Note: The statements, opinions, and data contained in all publications are solely those of the individual author(s) and contributor(s) and not of MDPI and/or the editor(s). MDPI and/or the editor(s) disclaim responsibility for any injury to people or property resulting from any ideas, methods, instructions, or products referred to in the content.

Article

Analysis of Adaptive Algorithms Based on Least-Mean-Square Applied to Hand Tremors Suppression Control

Rafael Silfarney Alves Araújo [1,†], Jessica Cristina Tironi [1,†], Wemerson Delcio Parreira [1,†,*], Renata Coelho Borges [2,†], Juan Francisco De Paz Santana [3,†,*] and Valderi Reis Quietinho Leithardt [4,5,†,*]

1 Laboratory of Embedded and Distributed Systems (LEDS), University of Vale do Itajaí (UNIVALI), Itajaí, SC 88302-901, Brazil
2 Federal University of Technology – Paraná (UTFPR); renatacoelho@utfpr.edu.br
3 Expert Systems and Applications Lab, Faculty of Science, University of Salamanca, Salamanca, Spain
4 COPELABS, Universidade Lusófona de Humanidades e Tecnologias, 1749-024 Lisbon, Portugal
5 VALORIZA, Research Center for Endogenous Resources Valorization, Instituto Politécnico de Portalegre, 7300-555 Portalegre, Portugal
* Correspondence: parreira@univali.br, valderi@ipportalegre.pt and fcofds@usal.es
† These authors contributed equally to this work.

Abstract: The increase in life expectancy, according to the World Health Organization, is a fact, and with it rises the incidence of age-related neurodegenerative diseases. The most recurrent symptoms are those associated with tremors resulting from Parkinson's Disease (PD) or Essential Tremors (ET). The main alternatives for the treatment of these patients are medication and surgical intervention, which sometimes have restrictions and side effects. Through computer simulations in Matlab software, this work investigates the performance of adaptive algorithms based on least mean squares (LMS) to suppress tremors in upper limbs, especially in the hands. The signals resulting from pathological hand tremors, related to PD, present components at frequencies that vary between 3 Hz and 6 Hz, with the more significant energy present in the fundamental and second harmonics, while physiological hand tremors, referred to ET, vary between 4 Hz and 12 Hz. We simulated and used these signals as reference signals in adaptive algorithms, Filtered-x Least Mean Square (Fx-LMS), Filtered-x Normalized Least Mean Square (Fx-NLMS), and a hybrid Fx-LMS&NLMS purpose. Our results showed that the vibration control provided by the Fx-LMS&LMS algorithm is the most suitable for physiological tremors. For pathological tremors, we have used a proposed algorithm with a filtered sinusoidal input signal, Fsinx-LMS, which presented the best results in this specific case.

Keywords: tremor suppression, adaptive algorithm, LMS, Parkinson

1. Introduction

According to the World Health Organization (WHO), people born in 2015 will have an average life expectancy of 20 years longer than people born 50 years ago in most of the world. Thus, there is also an expansion in the incidence of pathologies inherent to aging with increased longevity. In this sense, people over 60 are usually affected by neurological diseases that cause tremors – oscillatory involuntary movements in some parts of the body [1,2].

Tremors can be classified as tremors in action and tremors at rest [3]. Essential tremor (ET) is more predominantly action-related and affects the upper limbs, such as the hands and head, with frequency characteristics ranging from 4 Hz to 12 Hz [4]. This type of tremor can be bilateral or symmetric [5]. ET figures as one of the most prevalent neurological diseases in the world. Luis and Ferreira [6] estimated that about 1% of the world's population and approximately 6.4% of people over 65 years of age suffer from ET. On the other hand, tremors at rest, in most cases, are related to Parkinson's disease, which is the second principal pathology causing involuntary tremors. It occurs when the patient's limb is

© 2023 by the author(s). Distributed under a Creative Commons CC BY license.

Preprints (www.preprints.org) | NOT PEER-REVIEWED | Posted: 6 February 2023 doi:10.20944/preprints202302.0092.v1

completely relaxed and there is no anti-gravitational effort. In this case, unwanted movements are produced both in the lower limbs and in the upper limbs, in the frequency range between 3 Hz and 6 Hz [5]. People who suffer from PD and ET have difficulties performing simple everyday tasks such as eating and writing [5].

Conventional mitigating alternatives for these patients are linked to medication and surgical intervention. For treatment with the medication Levodopa, for example, it was observed that about 50% of patients, after 5 years of treatment, had some side effects such as agitation, hallucination, mood swings, and impulsivity [7,8], another form of treatment is surgical intervention.

Several devices have been developed in order to apply active, passive, and semi-active control techniques to help suppress unwanted movements arising from tremors, aiming to improve the life quality of people with PD and ET. Proportional, Integrative, and Derivative (PID) controllers have been used in recent research on vibration suppression, in which the controller act to minimize unwanted signal values in order to ensure that the system gain follows reference values [9]. In the proposed analysis in [10], for instance, a model of a human hand with four degrees of freedom was used, together with a piezoelectric actuator, showing the feasibility of using a PID controller to suppress PD vibrations. Such controllers can be fixed or can be updated according to some algorithm, such as adaptive techniques.

Our work brings a new contribution to discuss hand tremors suppression control with a comparison of adaptive techniques, more precisely Filtered-x based, for active vibration control applied to the suppression of movements arising from hand tremors. Among the advantages of the algorithms are faster convergence in ideal conditions and tracking capability. The comparisons account for complexity analysis, convergence time, and Mean Square Error (MSE) in the steady state. As is known, there are many challenges in research of this nature, especially in the difficulty of collecting and evaluating data on the intensity and frequency of tremors without the need to use invasive methods. In our analysis, we have used mathematical and computational models to analyze the attenuation effect. Therefore, tests in humans will not be considered in this study. The results presented in this work enable the performance analysis of the tested statistical learning algorithms involving Monte Carlo simulations.

The rest of this work is organized as follows. In Section 2 the mathematical models used to represent the hand tremor signal are presented and discussed. Section 3 presents the structure of the active vibration control and the filters used to compose the solution to the problem. Section 5 presents the results, as well as a discussion of the findings. In Section 6 final considerations and new directions for research in the area are presented.

1.1. Related publications

Active Vibration Control (AVC) consists of applying a force of opposite intensity to an external source of vibration. To reduce hand tremors, Turkistani [11] developed a tremor suppression prototype consisting of a flexible, portable glove. This prototype has a micro-electro-mechanical vibration simulation module based on an accelerometer-gyroscope embedded in the glove that mimics hand vibration. The vibration signal is collected and sent to a microcontroller. So that it can be processed and the vibration motors present in the fingers are activated to reduce the tremor.

Another method to eliminate human arm tremors was developed by Chuanasa and Songscho [12], who used the self-balancing technique. In this technique, a rotating unbalanced mass actuator was used to reproduce arm tremors with the same frequency range obtained from clinical sources. In addition to the composition of the counterbalance device designed to hold the dummy arm, a proportional derivative integral controller and an algorithm programmed in LabVIEW were used to control the rotary unbalanced mass actuator, anti-shaker, in the order to combat tremor.

The method used by Hosseini et al. [13] consists of the mathematical modeling of a system with 4 degrees of freedom of a biomechanical system that represents the human hand. Active control is done by combining a proportional and derivative controller and tested, via MATLAB-Simulink, in

Preprints (www.preprints.org) | NOT PEER-REVIEWED | Posted: 6 February 2023 doi:10.20944/preprints202302.0092.v1

three different types of actuators: piezoelectric, magnetic, and electric. Finally, the efficiency of each actuator was compared separately, with the piezoelectric actuator demonstrating greater efficiency in suppressing tremors such as those characteristics of Parkinson's disease.

As can be seen in Table 1, which presents a comparison of the techniques found in the literature that perform active vibration control, considering the last 7 years, there is no evidence that other publications have used adaptive filters to control vibrations associated to TE and PD. None of the techniques found showed signal acquisition.

Table 1. Comparative table of publications on the subject in the last 7 years.

Author	Technique	Control
[14]	Neural Network	Active
[15]	Adaptive Filter/Intern Control	Active
[13]	PID Control	Active
[12]	PID Control/Low-Pass Filter	Active
This paper	Adaptive Filters	Active

2. Mathematical models of tremors in upper limbs

In this work, a mathematical model of hand tremor similar to signal patterns obtained by clinical means and mathematically validated is used. Thus, the need to acquire signals in humans is eliminated. There are also advantages of using mathematical models such as easy identification, good spectral frequency resolution, and convenient use in embedded systems.

2.1. Physiological tremor model by time series

The characterization method used by Jakubowski et al. [16] in the distinction between essential, physiological, and parkinsonian tremors, consists of using higher-order statistics by Taylor series, in which third and fourth-order cumulants are implemented to describe the behavior of tremors. Furthermore, he claims that second-order Gaussian models are not able to distinguish between the three types of vibration patterns mentioned above.

The model presented by Zhang and Chu [17] consists of the simulation of physiological tremors in an outstretched hand loaded with a weight of 2.3 to 4.5 kg, for 60 seconds, using an autoregressive model of order $p = 3$, AR(3).

An autoregressive process of order p, AR(p), is given by:

$$\mathbf{x}(n) + \sum_{k=1}^{p} a_k \mathbf{x}(n-k) = z(n) \tag{1}$$

where a_k are the model coefficients and $z(n)$ is a white noise with Gaussian distribution with zero mean and variance σ^2. According to [18] the order that will produce the smallest error is $p = 3$.

2.2. Mathematical model of Parkinsonian tremor

Theoretically, the parkinsonian movement can be reconstituted by Fourier analysis with sinusoidal signals of multiple frequencies, where the amplitude and phase of the signal are determined by the spectrum [18]. In such wise, a tremor signal trm(n) is given by,

$$\begin{aligned} \text{trm(t)} = &\sin(f_1(t)) + \sin(f_2(t)) \\ &+ \sin(f_1(t)) \times \sin(f_2(t)) \end{aligned} \tag{2}$$

in which $f_1(t) \neq f_2(t) \in \mathbf{R}$.

The collaboration of Reeke [18], rests on a simple model, however very similar, to the real behavior of a vibration produced by the left wrist of a patient with Parkinson's. These models are both described

Preprints (www.preprints.org) | NOT PEER-REVIEWED | Posted: 6 February 2023 doi:10.20944/preprints202302.0092.v1

by the sum of two sinusoidal and by the multiplication of two sinusoidal frequencies different from those used in the sum.

The comparison in the time domain between the models by summing and sinusoidal multiplication by the real tremor recorded in a patient with resting tremor in the left wrist, in which sensors captured the supinator and patient's wrist pronator. In the representation of [18], it is possible to notice the accuracy of the mathematical model used and the representation in the frequency domain of the real tremor.

3. Vibration active control

Firstly, it is necessary to characterize the vibrational properties of the structure, i.e., to know how the parts of the structure vibrate, to understand and control the vibration. Thus, we enable anticipating vibration levels or determining the actions to control vibration. While passive noise control has been the predominant method used in tremor control applications, the search for ultimate vibration control has advanced to the extent that the use of active forces would be preferable to neutralize vibration. In this vibration control technic, called Active Vibration Control (AVC), the controller coefficients are constantly updated by an adaptive algorithm.

The AVC scheme, as highlighted in Figure 1, basically consists of the plant system[1], actuators, sensors, and controllers. For the tests carried out, two random white Gaussian signals with zero mean and unit variance, uncorrelated, are generated. In Figure 1 they are represented by the Noise Generator blocks and $x(n)$. The signal $x(n)$ is used to recognize the plant coefficients of the main loop (direct path) $W(z)$, on the other hand, the noise generator is an anti-signal generated in the loop (or secondary path) for recognizing the coefficients of the filter $S(z)$. The response of the input signal into the second loop in a finite impulse response (FIR) filter is used to filter the $\mathbf{x}(n)$ signal, which in turn feeds the adaptive algorithm, which acts to both recognize and estimate the coefficients of the main loop and to control the noise signal through the secondary loop.

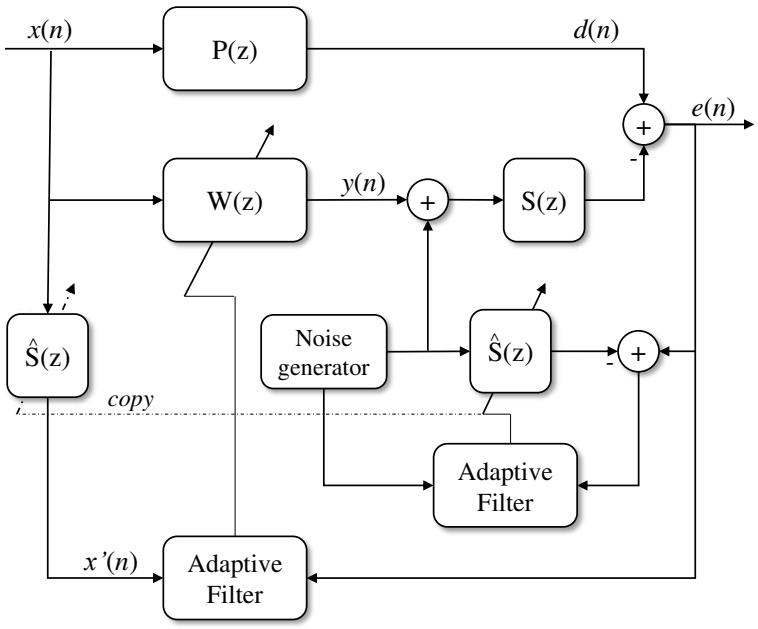

Figure 1. Block diagram of the basic functioning of an adaptive vibration control system.

[1] Coefficients that characterize the behavior of the dynamic system.

Preprints (www.preprints.org) | NOT PEER-REVIEWED | Posted: 6 February 2023 doi:10.20944/preprints202302.0092.v1

Active vibration control based on adaptive finite impulse response (FIR) filters typically introduces a conditional signal dispersion delay [19]. The reasons for these delays are geometric arrangements and computational time associated with the use of analog-to-digital converters (ADCs) and digital-to-analog converters (DACs). Delays represent a phase shift in periodic signals. These delays prevent instant feedback of signals from the Least-Mean Square (LMS) algorithm, for example. This can lead to instability and even divergence of the algorithms. Studies have presented a modification of the LMS algorithm, adjusting the underlying gradient descent algorithm [20–23] to work around this problem. The result is that any delays that occur can be fully compensated.

Different strategies are proposed for the use of the LMS algorithm in controlling noise and vibrations, usually taking into account that the LMS alone is not capable of attenuating unpredictable signals such as physiological tremors, for example. Active vibration control applications usually rely on the action of external elements, especially the analog-to-digital and digital-to-analog conversion processes, called here secondary path. In the presence of that processes, traditional algorithms such as LMS or RLS (Recursive Least Square), should not be applied, being the solution to this problem lying in filtering the input signal, using an estimation of the secondary path. The Filtered-x Least Mean Square (Fx-LMS) and its variations, which serve as the basis for this analysis, was an alternative proposed by Widrow et al. [24]. The strategy adopted also in [15] uses the Internal Model Control method (IMC[2]), together with the Fx-LMS algorithm to suppress noise and vibrations. Its results show robustness and segment of reference values.

In this work, some adaptive algorithms based on the least mean squares for active control of variable vibration systems will be evaluated. The framework also uses an auxiliary filter to improve the online estimation of the secondary path. The secondary path is represented by the transfer functions of the auxiliary filter and the controller, and its Finite Impulse Response (FIR) model is also estimated with an adaptive strategy.

3.1. Adaptive algorithms

The definition of an adaptive automaton, according to Widrow [25], consists of a system whose structure is adjustable in such a way that, based on a desirable value, its performance improves according to its contact with the applied environment. Thus, adaptive algorithms are employed where there is a constant change in their environment. They are usually applied in real-time systems, requiring a minimum calculation ratio per sample. These algorithms have a measurement process in order to get closer to the desired value. According to Aslam et al. [23] and Nascimento and Silva [26], adaptive filters can be seen as a disaggregating algorithm for mixing two signals and, for that, the reference values of one of the signals are essential.

3.1.1. Least-Mean Square (LMS) Algorithm

The Least Mean Square (LMS) algorithm is one of the most commonly used adaptive filtering algorithms due to its computational simplicity, ease of proving its efficiency in stationary environments, stable behavior when implemented with finite arithmetic precision, and because it does not need to estimate the approximation gradient of values offline [25,27]. The use of adaptive learning algorithms with statistical inference allows for estimating the behavior of systems that present characteristics that can change over time, as is the case of signals from hand tremors.

Figure 2, shows a diagram that helps in understanding the LMS. The vector $\mathbf{x} = (x_0, x_1, \ldots, x_n)$ represents the system input values, the vector $\mathbf{w} = (w_0, w_1, \ldots, w_n)$ refers to to the weights of the

[2] The internal model control systems are characterized by a control device composed by the controller and by a simulation of the process, the internal model.

Preprints (www.preprints.org) | NOT PEER-REVIEWED | Posted: 6 February 2023 doi:10.20944/preprints202302.0092.v1

algorithm, which will be updated at each iteration, $y(n)$ represents the output estimated by the weights and the input by:

$$y(n) = \mathbf{x}^\top(n)\,\mathbf{w}(n). \tag{3}$$

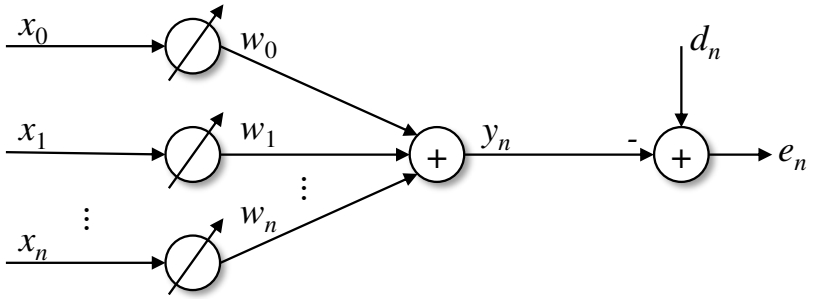

Figure 2. Weight diagram of the LMS algorithm [24].

The signal $d(n)$ is the signal to be approximated by the output $y(n)$ of the system and $e(n)$ represents the value of the error at instant n.

Thus,

$$e(n) = d(n) - y(n) \tag{4}$$

and therefore,

$$e(n) = d(n) - \mathbf{x}^\top(n)\,\mathbf{w}(n) \tag{5}$$

Taking the square value of the error (5) in order to minimize it, yields:

$$\begin{aligned} e^2(n) = d^2(n) &- 2\,d(n)\,\mathbf{x}^\top(n)\,\mathbf{w}(n) \\ &+ \mathbf{x}(n)\,\mathbf{w}^\top(n)\,\mathbf{w}(n)\,\mathbf{x}^\top(n). \end{aligned} \tag{6}$$

The Mean Square Error (MSE) is obtained from the calculation of the mean operator, $E[.] = \xi(n)$, in (6),

$$\begin{aligned} \xi(n) = E[d^2(n)] &- 2\,E[d(n)\mathbf{x}^\top(n)]\mathbf{w}(n) \\ &+ \mathbf{w}^\top(n)E[\mathbf{x}(n)\mathbf{x}^\top(n)]\mathbf{w}(n) \end{aligned} \tag{7}$$

or

$$\xi(n) = E[d^2(n)] - 2\,\mathbf{p}_{xd}^\top(n)\,\mathbf{w}(n) + \mathbf{w}^\top(n)\mathbf{R}_{xx}\mathbf{w}(n) \tag{8}$$

where $\mathbf{p}_{xd} = E[d(n)\mathbf{x}(n)]$ is the cross-correlation vector of input and output signals and $\mathbf{R}_{xx} = E[\mathbf{x}(n)\mathbf{x}^\top(n)]$, known as the deterministic autocorrelation matrix of the input signal.

It is observed that from (8), the MSE is given as a function of the weights, so the weights must be adjusted to reduce the error. This weight adjustment falls on a negative gradient in the decay rate of the root mean square error with respect to the weight adjustment, as shown by applying the derivative to (7):

$$\frac{d\xi(n)}{d\mathbf{w}(n)} = -2d(n)\mathbf{x}(n) + 2\mathbf{x}(n)\mathbf{x}^\top(n)\mathbf{w}(n) = \nabla(n) \tag{9}$$

and

$$\nabla(n) = -2\mathbf{x}(n)[d(n) - \mathbf{x}^\top(n)\mathbf{w}(n)]. \tag{10}$$

Substituting Equation (5) into Equation (10), we have:

$$-\nabla(n) = 2\,\mathbf{x}(n)\,e(n) \tag{11}$$

Preprints (www.preprints.org) | NOT PEER-REVIEWED | Posted: 6 February 2023 doi:10.20944/preprints202302.0092.v1

The matrix $\mathbf{R}_{xx}$ is a positive definite matrix and the solution, $\mathbf{w}_o$, which minimizes the MSE, commonly known as the Wiener solution is given by:

$$\mathbf{w}_o = \mathbf{R}_{xx}^{-1}(n)\mathbf{p}(n). \tag{12}$$

The weight update equation for the LMS algorithm is given by:

$$\mathbf{w}(n+1) = \mathbf{w}(n) + \mu[-\nabla(n)]. \tag{13}$$

where μ is the adaptation step of the algorithm. The smaller this adjustment the more precise the adaptation, however a very small value of μ can result in a slower response of the adaptation system due to the high number of points.

Substituting the values of (11) in (13) yields:

$$\mathbf{w}(n+1) = \mathbf{w}(n) + \mu\mathbf{x}(n)e(n). \tag{14}$$

3.1.2. Normalized Least Mean Square (NLMS) Algorithm

The Normalized Least Mean Square (NLMS) Algorithm is a variation of the conventional LMS. In the LMS, the value of the learning step μ is a fixed value, while in the NLMS this value is variable over time, in the form $\mu(n)$ [28].

Thus, in the case of NLMS, (14) can be rewritten as:

$$\mathbf{w}(n+1) = \mathbf{w}(n) + \mu(n)\mathbf{x}(n)e(n). \tag{15}$$

It is then necessary to define the posterior error since the adaptive step value is variable. Thus

$$e_p = d(n) - \mathbf{w}^\top(n+1)\,\mathbf{x}(n). \tag{16}$$

and substituting (15) into (16), yields:

$$e_p = [1 - \mathbf{x}^\top(n)\mathbf{x}(n)\mu(n)]\,e(n). \tag{17}$$

The value of $\mu(n)$, which approximates the error value to its minimum, is given by:

$$\mu(n) = \frac{1}{||\mathbf{x}(n)||^2} \tag{18}$$

in which $||\mathbf{x}(n)||^2$ is the ℓ_2-norm, i.e.,

$$||\mathbf{x}(n)||^2 = \sum_{i=0}^{M-1} |\mathbf{x}(n-i)|^2. \tag{19}$$

Replacing (18) in (15), yields

$$\mathbf{w}(n+1) = \mathbf{w}(n) + \frac{1}{||\mathbf{x}(n)||^2}\,\mathbf{x}(n)e(n). \tag{20}$$

Expression (19) leads to an important regulation to determine the variation of the instantaneous squared error.

Now, let us introduce a positive real scaling factor μ in (18) in the same way of [29]. This scaling factor is important to control the change in the tap-weight vector from one interaction to the next without changing the direction of the vector. Hence, the updating weights in the NLMS is given by:

$$\mathbf{w}(n+1) = \mathbf{w}(n) + \frac{\mu}{||\mathbf{x}(n)||^2}\mathbf{x}(n)e(n). \tag{21}$$

Preprints (www.preprints.org) | NOT PEER-REVIEWED | Posted: 6 February 2023 doi:10.20944/preprints202302.0092.v1

Thus, we have a rate of convergence that is potentially faster than that of the LMS. Let us denote $\mu(n)$ by μ from this moment for simplification.

3.1.3. Filtered-X Least Mean Square (Fx-LMS) Algorithm

For real-time active noise control applications, the LMS algorithm, due to the long delay, is not the most suitable algorithm, as the noise at the system input can generate instability. As an alternative to this problem, Widrow [24] presented as a solution an algorithm that has an estimated signal input, in which the reference signal is adaptively filtered and compared with the input signal, obtaining the estimated signal. The Fx-LMS algorithm is normally used to update the adaptive filter, as shown in Figure 3.

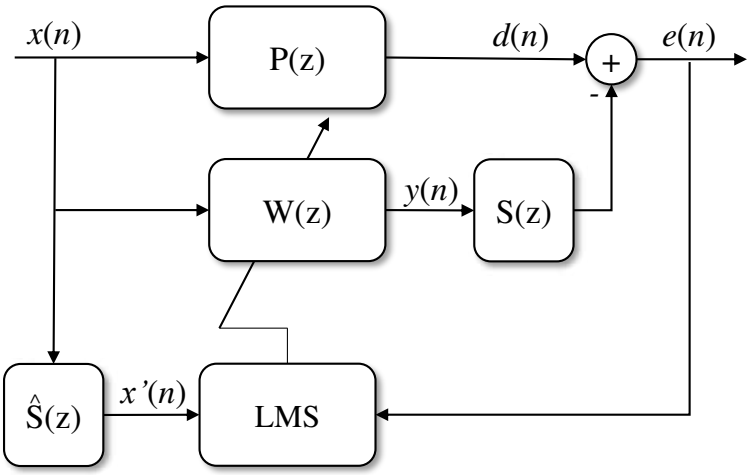

Figure 3. Block diagram of Fx-LMS algorithm.

Analysis of the Fx-LMS convergence with stochastic signals on entry is presented in [30] considering a moving average process. In this case, $P(z)$ is the primary path plan, and $\widehat{\mathbf{S}}(z)$ represents the estimated value of $\mathbf{S}(z)$, its secondary path plan. Thus, the estimate of $\mathbf{S}(z)$ is given by:

$$\widehat{\mathbf{S}}(z) = \sum_{q}^{Q-1} \frac{\mathbf{S}_q}{Z^q}. \tag{22}$$

The equation that represents the error of the system, in the time domain, can be described as:

$$e(n) = d(n) - \sum_{q}^{Q-1} \mathbf{S}_q y(n-q). \tag{23}$$

Assuming the output $y(n) = \mathbf{w}^\top(n)\mathbf{x}(n)$, as well as in (5), substituting in (23), you get an error equation:

$$e(n) = d(n) - \sum_{q}^{Q-1} \mathbf{S}_q \mathbf{x}^\top(n-q)\mathbf{w}(n-q). \tag{24}$$

Using a methodology analogous to Wiener's optimal solution, an expression similar to (12) is obtained, but with filtered values, given by:

$$\mathbf{w}_* = {\mathbf{R}_f}^{-1}(n)\mathbf{p}_f(n) \tag{25}$$

where $\mathbf{w}_*$ denotes the optimal vector of weights, $\mathbf{R}_f(n)$ denotes the correlation matrix of filtered entries, and $\mathbf{p}_f(n)$ represents the cross-correlation between the filtered input and the desired signal.

Preprints (www.preprints.org) | NOT PEER-REVIEWED | Posted: 6 February 2023 doi:10.20944/preprints202302.0092.v1

The expression for the input $\mathbf{x}_f(n)$ is obtained by filtering $\mathbf{x}(n)$ using $\widehat{\mathbf{S}}(n)$:

$$\mathbf{x}_f(n) = \sum_{q}^{Q-1} \mathbf{S}_q \mathbf{x}(n-q). \tag{26}$$

The optimal value of the error measured by substituting (25) and (26) in (24), is given by:

$$e_*(n) = d(n) - \mathbf{w}_*^\top(n)\mathbf{x}_f(n). \tag{27}$$

From (27) the weight vector that updates the Fx-LMS algorithm is:

$$\mathbf{w}(n+1) = \mathbf{w}(n) + \mu e(n)\mathbf{x}_f(n) \tag{28}$$

where μ, as in the LMS, is the convergence step of the algorithm.

4. Simulation configurations

In this section, simulation configurations are presented for comparison of adaptive algorithms to control tremors in upper limbs. The Fx-LMS and its variations, which serve as the basis for this analysis, was an alternative to solve the problem of traditional algorithms such as LMS and RLS [24].

Based on the results, it is possible to analyze the behavior of the Fx-LMS and Fx-NLMS algorithms in the control of physiological tremors in a mesh that considers the online adjustment of the secondary path, eliminating the need for a fitting step during the calibration period. In addition, considering the characteristics of these algorithms, the behavior for a hybrid approach is also evaluated, being titled Fx-LMS&NLMS. This is a suggestion of changing the traditional format of the algorithms mentioned above.

In a second approach, control is applied to Parkinson's tremors. In this case, the behavior of the Fx-LMS algorithm with sinusoidal input was considered, which will be denoted by Fsinx-LMS, an algorithm that is also a suggestion and adaptation of this analysis.

The design parameters (step-sizes) were defined by exhaustive trials, considering a faster fit for the secondary path for both controllers. The following value ranges were analyzed: 0.7×10^{-3} to 0.1 in steps of 10^{-4}.

4.1. Simulation setup for physiological tremors control

The model used to simulate physiological tremors in this work is based on the study by Zhang and Chu [17], in which the weight coefficients of the model described by an AR process were obtained through filtering by the Levinson-Durbin algorithm[3], presented in 2.1. The analysis of the algorithm was performed by the minimum MSE, which presented a residual error of 5×10^{-3} for a model of the third order.

The coefficients used in the AR(3) model to reproduce physiological tremor were $P(z) = [-2.7288\ 2.5774\ 0.8342]^\top$. To control the physiological tremors signal, the $S(z)$ plant must be a model proportional to $P(z)$, in this work we have used $S(z) = 0.1\,P(z)$. A white Gaussian signal, with zero mean and unitary variance, was used to produce the desired signal $d(n)$ shown in Figure 1.

The convergence step of the analyzed algorithms was maintained for all algorithms, as well as the number of interactions. After exhaustive tests, it was decided to use $\mu = 0.1$ in the direct path and $\mu = 10^{-2}$ in the secondary path. In this way, the best results were obtained for both algorithms and scenarios.

---

[3] More details on this approach can be found in [17,31]

Preprints (www.preprints.org) | NOT PEER-REVIEWED | Posted: 6 February 2023 doi:10.20944/preprints202302.0092.v1

4.2. Simulation setup for pathological tremors control

The model defined in Section 2.2, Eq. (2) – which is a synthetic signal similar to Parkinson's tremor – was used in order to generate the synthetic signal. This signal simulates the tremor of Parkinson's disease, as can be seen in Figure 4. The frequency values used for the sinusoid sum were 5.2 Hz and 4.6 Hz.

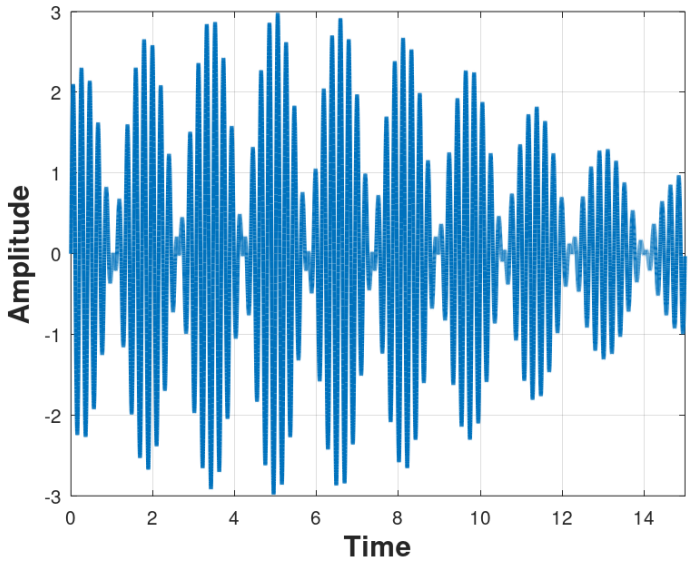

Figure 4. Parkinson's tremor signal in the time domain.

Figure 5 represents the Fourier transform of the synthetic Parkinson's tremor signal shown in Figure 4. Note the occurrence of the peaks at approximately 4.5 Hz and 5.5 Hz.

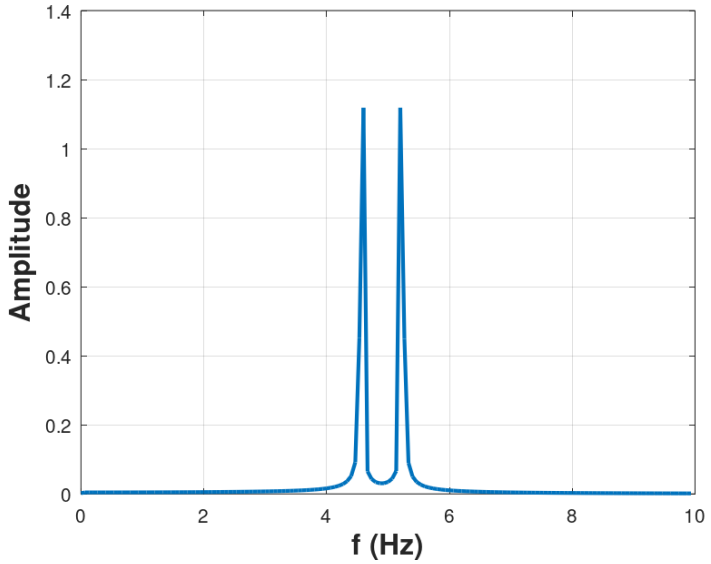

Figure 5. Parkinson's tremor signal in the frequency domain.

Unlike linear systems which can be uniquely identified by their impulse response, nonlinear systems need to additional steps. In this way, we require nonlinear processing. Therefore, we need a transformation in input space to guarantee the modeling of the nonlinear part of the system.

The linear filter is $\mathbf{S}(z) = [0.51423\ 0.92868]^\top$. The desired signal $d(n)$ was generated according (2). The input signal $x(n)$ is the white Gaussian noise transformed by sinusoids. We clarify that, in this case, P(z) is not displayed because it is a non-linear system composed of the sum of sinusoids. The

Preprints (www.preprints.org) | NOT PEER-REVIEWED | Posted: 6 February 2023 doi:10.20944/preprints202302.0092.v1

need to change the signals of the primary and secondary paths by sinusoids was due to the nonlinear characteristic of the desired signal $d(n)$. This is an adaptation, called here the FsinX-LMS algorithm, given that the dynamics of the Parkinson's disease signal are non-linear and deterministic. A Gaussian white noise generator would not be able to generate a control signal for Parkinson's tremors, given its linear nature. We have used the step-size, $\mu = 0.05$ in the primary path and $\mu = 0.08$ in the secondary path.

5. Results

This section presents the reporting of the results of the experiments performed. First, 5.1, the performance of the adaptive filter for physiological tremors (essential tremors) using Fx-LMS, Fx-NLMS and a hybrid of Fx-LMS&NLMS are shown. The second experiment comprises the results for the named Fsinx-LMS algorithm applied in the control of pathological tremors (related to Parkinson's disease), 5.2.

5.1. Simulation result of physiological tremors control

The results of this research will be presented by comparing the algorithms Fx-LMS, Fx-NLMS, and LMS. In the first and second scenarios, the adaptive filters (Figure 1) were updated using the Fx-LMS and Fx-NLMS algorithms, respectively. In the third scenario, a hybrid condition was considered, in which the adaptive filter corresponding to the direct path is updated by the Fx-LMS algorithm and the filter in the secondary path is updated by the Fx-NLMS algorithm. The basic difference between the three scenarios is in the normalization of the error signal of the main and secondary loops. In Scenario 1, Fx-LMS, there is no normalization of the error signal data of the algorithm loops. In Scenario 2, Fx-NLMS, there is data normalization in both the main and secondary mesh. In Scenario 3, Fx-LMS&NLMS, the normalization is done only in the secondary path.

5.1.1. Scenario 1 (Fx-LMS)

The behavior of the Fx-LMS algorithm (Scenario 1) in the active control of physiological tremor vibration is shown in Figure 6. The steady state is reached after approximately 4000 samples. Figure 7 shows the result of the normalized mean square error (MSE) signal intensity, with a final mean value of -22 dB.

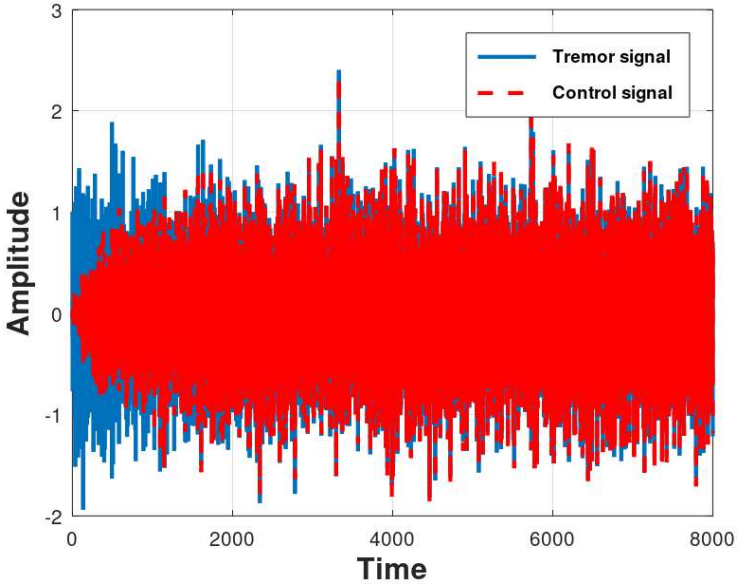

Figure 6. Control evaluation results produced by the Fx-LMS algorithm for 30 runs of a Monte Carlo simulation.

Preprints (www.preprints.org) | NOT PEER-REVIEWED | Posted: 6 February 2023 doi:10.20944/preprints202302.0092.v1

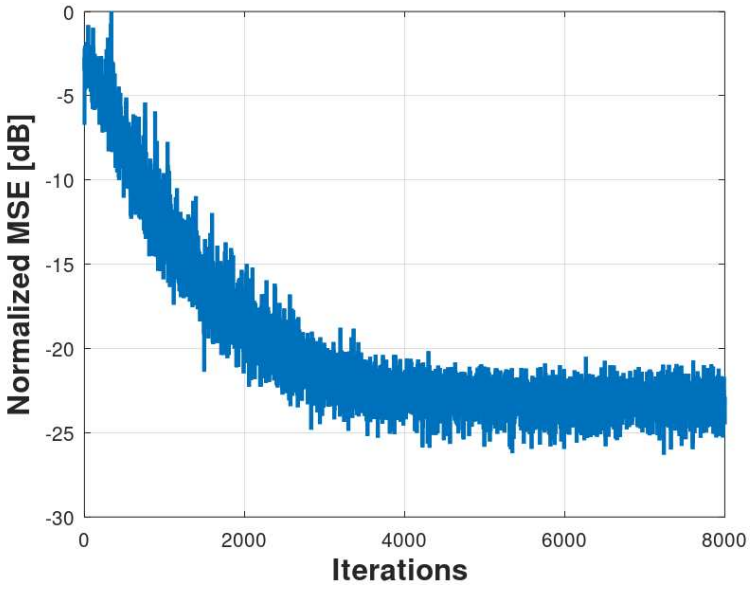

Figure 7. Normalized-MSE results produced by the Fx-LMS algorithm for 30 runs of a Monte Carlo simulation.

5.1.2. Scenario 2 (Fx-NLMS)

The Fx-NLMS algorithm has normalized data in both the main and secondary loops and its result for controlling the physiological tremor signal is illustrated by Figure 8. In this case, approximately 4500 samples are needed for the control signal to converge, following the reference values, and it is enough to minimize the tremors. Figure 9 shows the results for the normalized mean squared error signal data. As in scenario 1, the squared error, after convergence of the coefficients reaches an average value of -22 dB of attenuation.

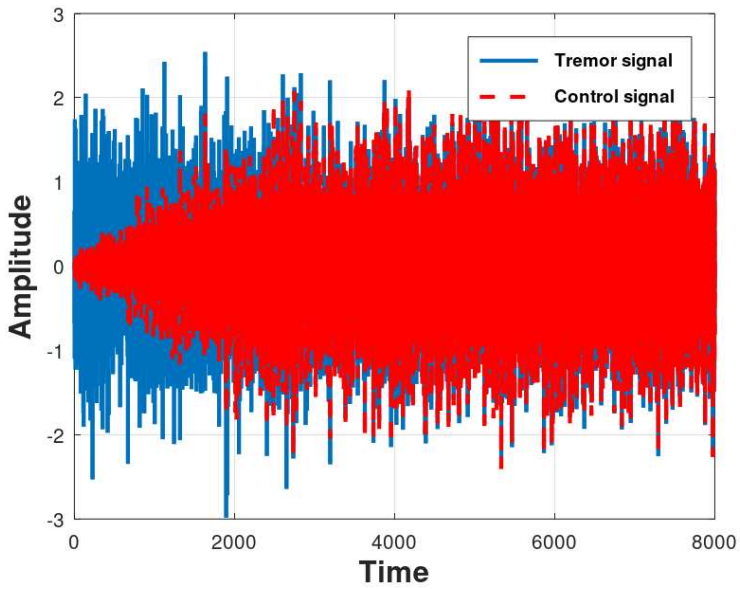

Figure 8. Control evaluation results produced by the Fx-NLMS algorithm for 30 runs of a Monte Carlo simulation.

Preprints (www.preprints.org) | NOT PEER-REVIEWED | Posted: 6 February 2023 doi:10.20944/preprints202302.0092.v1

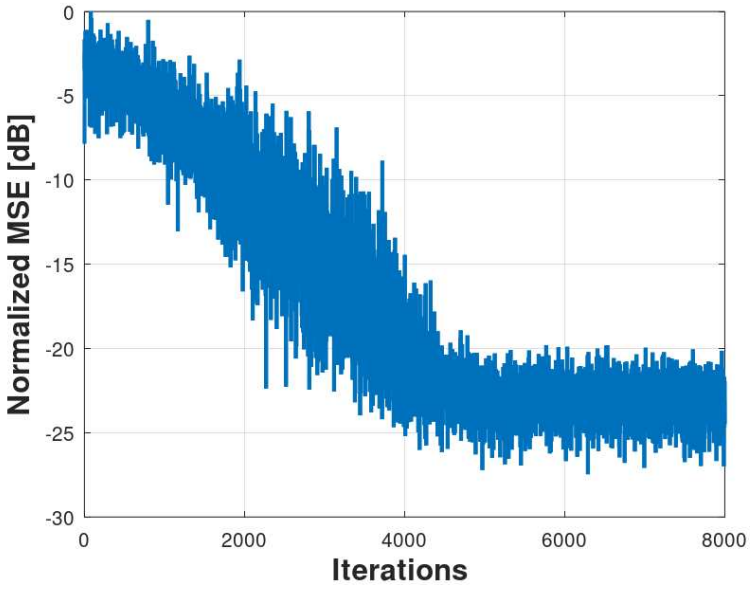

Figure 9. Normalized-MSE results produced by the Fx-NLMS algorithm for 30 runs of a Monte Carlo simulation.

5.1.3. Scenario 3 (Fx-LMS&NLMS)

In scenario 3, hybrid, the control structure uses the Fx-LMS&NLMS algorithms, which have normalized data in the secondary loop error. This arrangement of algorithms is a suggestion of this work regarding a change in the normalization of the secondary path only. This combination enabled a gain in performance. Figure 10 shows the control result of the algorithm, where the steady state is reached with approximately 4000 samples and reaches an average value of -28 dB of attenuation.

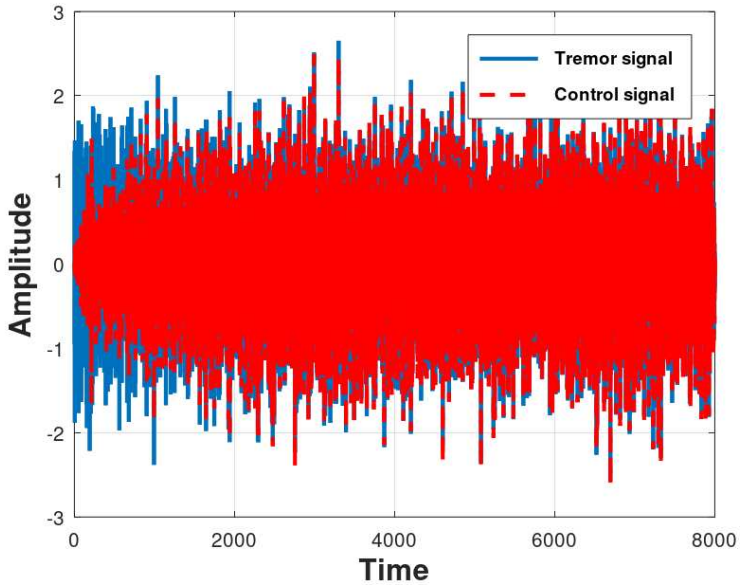

Figure 10. Control evaluation by the Fx-LMS&NLMS algorithm for 30 runs of a Monte Carlo simulation.

Preprints (www.preprints.org) | NOT PEER-REVIEWED | Posted: 6 February 2023 doi:10.20944/preprints202302.0092.v1

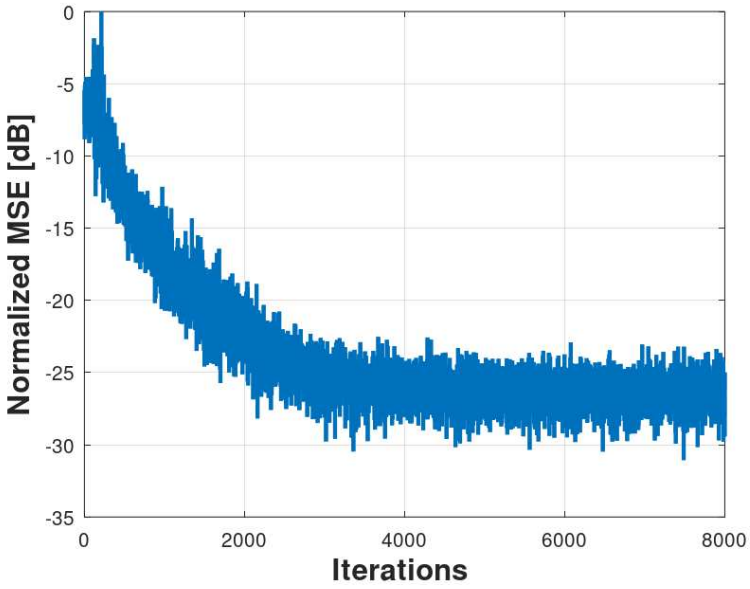

Figure 11. Normalized MSE results produced by the Fx-LMS&NLMS algorithm for 30 runs of a Monte Carlo simulation.

5.1.4. General comparison of Fx-LMS, Fx-NLMS, and Fx-NLMS&LMS

The Fx-LMS and Fx-NLMS algorithms, implemented in scenarios 1 and 2, respectively, presented a similar mean squared error attenuation level. The most relevant difference in behavior occurred in the convergence times of each one of them. The Fx-LMS algorithm reached an error of -22 dB in 4000 samples, 500 less than the time obtained in scenario 2.

The Fx-LMS&NLMS algorithm, implemented in scenario 3, proved to be faster if compared to NLMS algorithm, requiring 4000 samples to carry out the active control, a reduction of 30% compared to scenarios 1 and 2. This result can be attributed to fast response due to normalized filtering in the modeling of the only plant of $\mathbf{S}(z)$. This comparison can be seen in Figure 12.

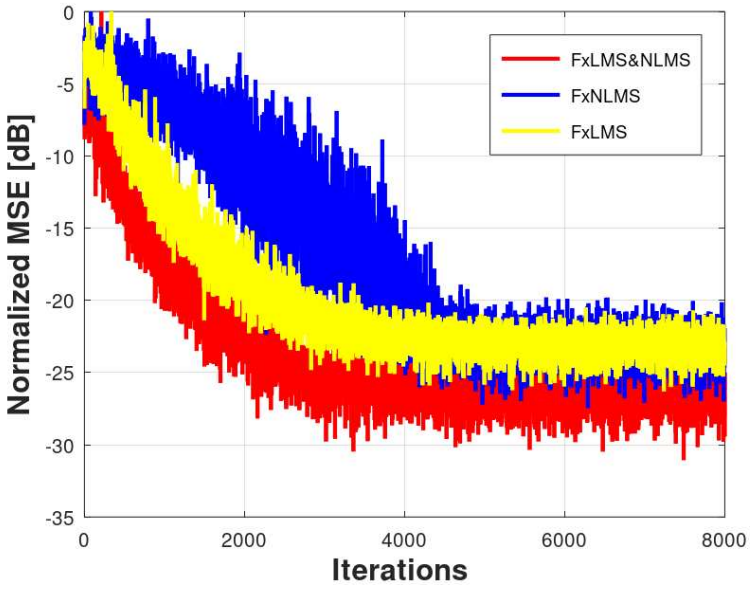

Figure 12. Comparison of the normalized MSE behavior averaged over 30 runs. Ragged curves (yellow): Monte Carlo simulation of Fx-LMS. Ragged curves (blue): Monte Carlo simulation of Fx-NLMS. Ragged curves (red): Monte Carlo simulation of Fx-LMS&NLMS.

Preprints (www.preprints.org) | NOT PEER-REVIEWED | Posted: 6 February 2023 doi:10.20944/preprints202302.0092.v1

It is clear that an analysis in terms of computational complexity is necessary for a cost-benefit assessment. But, in a scenario where there is no complexity restriction, Fx-LMS&NLMS achieved faster convergence.

Table 2 presents more clearly the final comparison of the results in terms of the number of iterations and the amplitude and attenuation of the tremors in terms of square mean errors.

Table 2. Comparative Table of Results.

Algorithm	Samples	MSE
Fx-LMS	4000	-22 dB
Fx-NLMS	4500	-22 dB
Fx-LMS&NLMS	4000	-28 dB

5.2. Simulation result of pathological tremors control

The dynamics of parkinsonian tremor are non-linear, deterministic, and chaotic [32]. This is a totally different way of controlling what was previously shown with algorithms based on zero-mean and unitary variance Gaussian noise signals.

The control signal generated by the Fsinx-LMS algorithm will always try to follow the non-linearity and non-stationary nature of the tremor signal similar to that produced by the Parkinson tremor signal, as illustrated in Figure 13. Analogous dynamics can be founded in [33,34]. Other solutions involving applied algorithms there are other scenarios with metrics and parameters can be viewed at [35,36]. In this way, the algorithm learns the dynamics of the tremor signal until its pattern changes and the algorithm needs to readapt itself, converging for the new coefficients. The MSE shown in Figure 14 represents the operation of the adaptive algorithm. There is a high MSE initially, due to delay of the control system, until the error decreases drastically when the control signal follows the desired signal and the vibration pattern changes, and so the MSE increases again. This cycle repeats itself indefinitely. Unlike what happened in Section 5.1, it is not possible to obtain a steady-state error since the MSE is always trying to adapt to the behavior of the system that changes with a periodic characteristic. But, it is possible to notice that the attenuation lies around 14 dB.

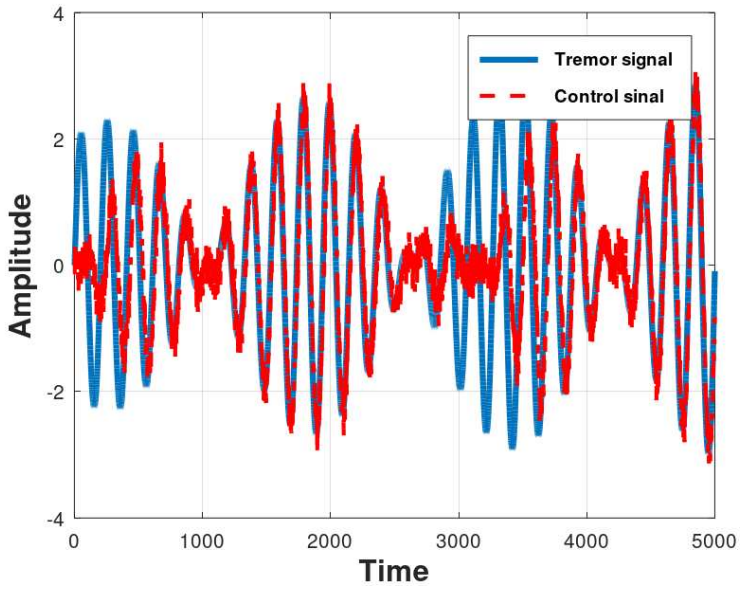

Figure 13. Control evaluation results produced by the FsinX-LMS algorithm for 30 runs of a Monte Carlo simulation.

Preprints (www.preprints.org) | NOT PEER-REVIEWED | Posted: 6 February 2023 doi:10.20944/preprints202302.0092.v1

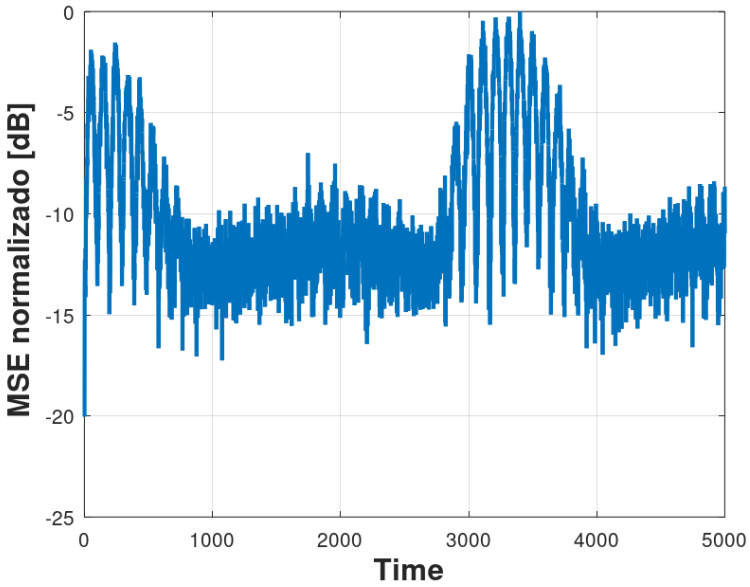

Figure 14. Normalized-MSE results produced by the FsinX-LMS algorithm for 30 runs of a Monte Carlo simulation.

6. Conclusions

Adaptive algorithms usually have a complex nature, which demands a need for knowledge of statistics, mathematics, signal processing, and computing tools. This work sought to collaborate by presenting a discussion about these algorithms and a sequence of scientific tests that would allow their application in problems of Mechanical, Electronic, Computing, and Biomedical Engineering.

The bibliographic review allowed the construction and survey of the necessary concepts for the application of adaptive filtering techniques in order to actively control vibration. In addition, information about the problem to be solved and knowledge of the vibratory patterns are mentioned here. This search was based on mathematical models, avoiding the need for invasive data collection on patients.

From the obtained results it was noticed a great sensitivity to the model, the family of algorithms, and the parameters used. Active control of physiological and Parkinsonian tremors was presented using algorithms from the adaptive LMS family. The Fx-LMS&NLMS Algorithm showed the best response among the algorithms used in this research. Its difference from the others, Fx-LMS and Fx-NLMS, is only in the number of iterations. The algorithm that obtained the slowest response was the result of non-normalization in the primary mesh, where the plant of the system is initially recognized. The Fx-LMS algorithm is traditionally used in stroke, and can, in a way, serve as a parameter in relation to its variations, per hour used in the control of physiological tremors.

To provide active control of Parkinsonian tremors, the Fsinx-LMS algorithm was presented. Derived from Fx-LMS, this algorithm has only one additional block for the non-linearization of generated random signals, producing a random phase sinusoid. This was necessary so that the non-linearities of the model could be mapped by the adaptive system. It shows that there is a way to control deterministic and non-linear tremors, such as the tremor of Parkinson's disease, through LMS-type algorithms, provided that the generated signals are non-linear.

This study can be extended to other types of algorithms, especially for Parkinsonian tremors. In this case, kernelized algorithms can produce better results in systems with non-linear characteristics present in models that replicate this type of pathology. These algorithms have been applied by the scientific community and produced good results. Other approaches for estimating nonlinear systems can yet be considered, such as [33,34,37–39].

Preprints (www.preprints.org) | NOT PEER-REVIEWED | Posted: 6 February 2023 doi:10.20944/preprints202302.0092.v1

In addition, an implementation in embedded devices, DSP boards (Digital Signal Processor) can improve the understanding of the behavior of these algorithms in a practical scenario, which would later serve as a basis for the development of an electronic prototype with the embedded technology composed of a sensor and actuator to provide active control.

Author Contributions: Conceptualization, R.S.A., W.D.P., and R.C.B; methodology, R.S.A, and W.D.P.; analysis, R.S.A, J.C.T, W.D.P., and R.C.B; writing—original draft preparation, R.S.A, W.D.P, R.C.B, and J.C.T.; writing—review and editing, R.S.A, V.R.Q.L., W.D.P., J.F.d.P.S, and R.C.B All authors have read and agreed to the published version of the manuscript.

Funding: Not applicable.

Institutional Review Board Statement: Not applicable.

Informed Consent Statement: Not applicable.

Data Availability Statement: Not applicable.

Acknowledgments: Fundação para a Ciência e a Tecnologia, I.P. (Portuguese Foundation for Science and Technology) by the project UIDB/05064/2020 (VALORIZA–Research Centre for Endogenous Resource 764 Valorization), and Project UIDB/04111/2020, ILIND–Instituto Lusófono de Investigação e Desenvolvimento, under project COFAC/ILIND/ COPELABS/3/2020.

Conflicts of Interest: The authors declare no conflict of interest.

Abbreviations

The following abbreviations are used in this manuscript:

Active Vibration Control	AVC
Analog-to-digital converters	ADC
Digital Signal Processor	DSP
Digital-to-analog converters	DAC
Essential Tremors	ET
Filtered-x Least Mean Square	Fx-LMS
Filtered-x Normalized Least Mean Square	Fx-NLMS
Finite Impulse Response	FIR
Internal Model Control	IMC
Least Mean Square	LMS
Mean Square Error	MSE
Normalized Least Mean Square	NLMS
Parkinson's Disease	PD
Proportional, Integrative, and Derivative	PID
Recursive Least Square	RSL
World Health Organization	WHO

References

1. Findley, L.J. Classification of tremors. *Journal of Clinical Neurophysiology* **1996**, *13*, 122–132. doi:10.1097/00004691-199603000-00003.
2. Aryal, S.; Skinner, T.; Bridges, B.; Weber, J.T. The pathology of Parkinson's disease and potential benefit of dietary polyphenols. *Molecules* **2020**, *25*, 4382. doi:10.3390/molecules25194382.
3. Bhatia, K.P.; Bain, P.; Bajaj, N.; Elble, R.J.; Hallett, M.; Louis, E.D.; Raethjen, J.; Stamelou, M.; Testa, C.M.; Deuschl, G.; others. Consensus Statement on the classification of tremors. from the task force on tremor of the International Parkinson and Movement Disorder Society. *Movement Disorders* **2018**, *33*, 75–87. doi:10.1002/mds.27121.
4. Louis, E.D.; Ottman, R. Essential tremor. In *Genetics of Movement Disorders*; Elsevier, 2003; pp. 353–363. doi:10.1001/archneurol.2009.217.
5. Lenka, A.; Jankovic, J. Tremor syndromes: an updated review. *Frontiers in Neurology* **2021**, *12*. doi:10.3389/fneur.2021.684835.

Preprints (www.preprints.org) | NOT PEER-REVIEWED | Posted: 6 February 2023 doi:10.20944/preprints202302.0092.v1

6. Louis, E.D.; Ferreira, J.J. How common is the most common adult movement disorder? Update on the worldwide prevalence of essential tremor. *Movement Disorders* **2010**, *25*, 534–541.
7. Voon, V.; Napier, T.C.; Frank, M.J.; Sgambato-Faure, V.; Grace, A.A.; Rodriguez-Oroz, M.; Obeso, J.; Bezard, E.; Fernagut, P.O. Impulse control disorders and levodopa-induced dyskinesias in Parkinson's disease: an update. *The Lancet Neurology* **2017**, *16*, 238–250.
8. Sweet, R.D.; McDowell, F. Five years' treatment of Parkinson's disease with levodopa: therapeutic results and survival of 100 patients. *Annals of internal medicine* **1975**, *83*, 456–463.
9. Lekshmi, A.; Ramachandran, K. Parkinson's tremor suppression using active vibration control method. IOP Conference Series: Materials Science and Engineering. IOP Publishing, 2019, Vol. 577, p. 012056. doi:10.1088/1757-899X/577/1/012056.
10. Kazi, S.; Mailah, M.; Zain, Z.M. Suppression of hand postural tremor via active force control method. *Manufacturing Engineering, Automatic Control and Robotics* **2014**.
11. Turkistani, A. Development of an Effective Portable and Flexible Glove for Hand Tremor Suppression **2017**.
12. Chuanasa, J.; Songschon, S. Essential tremor suppression by a novel self-balancing device. *Prosthetics and orthotics international* **2015**, *39*, 219–225.
13. Hosseini, S.; Al-Jumaily, A.; Abboud, S.A. Active force control system for hand tremor suppression by different actuators. 2016 5th International Conference on Electronic Devices, Systems and Applications (ICEDSA). IEEE, 2016, pp. 1–4.
14. Ibrahim, A.; Zhou, Y.; Jenkins, M.E.; Trejos, A.L.; Naish, M.D. Real-Time Voluntary Motion Prediction and Parkinson's Tremor Reduction Using Deep Neural Networks. *IEEE Transactions on Neural Systems and Rehabilitation Engineering* **2021**, *29*, 1413–1423.
15. Kim, B.; Yoon, J.Y. Modified LMS strategies using internal model control for active noise and vibration control systems. *Applied Sciences* **2018**, *8*, 1007.
16. Jakubowski, J.; Kwiatos, K.; Chwaleba, A.; Osowski, S. Higher order statistics and neural network for tremor recognition. *IEEE Transactions on Biomedical Engineering* **2002**, *49*, 152–159.
17. Zhang, J.; Chu, F. Real-time modeling and prediction of physiological hand tremor. Proceedings.(ICASSP'05). IEEE International Conference on Acoustics, Speech, and Signal Processing, 2005. IEEE, 2005, Vol. 5, pp. v–645.
18. Reeke, G.N.; Poznanski, R.R.; Lindsay, K.A.; Rosenberg, J.R.; Sporns, O. *Modeling in the neurosciences: from biological systems to neuromimetic robotics*; CRC Press, 2005.
19. Dabis, H.; Moir, T. Least mean squares as a control system. *International Journal of Control* **1991**, *54*, 321–335.
20. Elliott, S.; Stothers, I.; Nelson, P. A multiple error LMS algorithm and its application to the active control of sound and vibration. *IEEE Transactions on Acoustics, Speech, and Signal Processing* **1987**, *35*, 1423–1434.
21. Song, P.; Zhao, H. Filtered-x least mean square/fourth (FXLMS/F) algorithm for active noise control. *Mechanical Systems and Signal Processing* **2019**, *120*, 69–82.
22. Martinek, R.; Rzidky, J.; Jaros, R.; Bilik, P.; Ladrova, M. Least mean squares and recursive least squares algorithms for total harmonic distortion reduction using shunt active power filter control. *Energies* **2019**, *12*, 1545.
23. Aslam, M.S.; Shi, P.; Lim, C.C. Robust Active Noise Control Design by Optimal Weighted Least Squares Approach. *IEEE Transactions on Circuits and Systems I: Regular Papers* **2019**.
24. Widrow, B.; Glover, J.R.; McCool, J.M.; Kaunitz, J.; Williams, C.S.; Hearn, R.H.; Zeidler, J.R.; Dong, J.E.; Goodlin, R.C. Adaptive noise cancelling: Principles and applications. *Proceedings of the IEEE* **1975**, *63*, 1692–1716.
25. Widrow, B.; Stearns, S.D. Adaptive Signal Processing Prentice-Hall. *Englewood Cliffs, NJ* **1985**.
26. Nascimento, V.H.; Silva, M.T. Adaptive filters. In *Academic Press Library in Signal Processing*; Elsevier, 2014; Vol. 1, pp. 619–761.
27. Paulo, S.D. *Adaptive filtering: algorithms and practical implementation*; Springer US, 2013.
28. Poularikas, A.D. *Adaptive filtering: Fundamentals of least mean squares with MATLAB®*; CRC Press, 2017.
29. Sayed, A.H. *Fundamentals of adaptive filtering*; John Wiley & Sons, 2003.
30. Ardekani, I.T.; Abdulla, W.H. Theoretical convergence analysis of FxLMS algorithm. *Signal Processing* **2010**, *90*, 3046–3055.
31. Brockwell, P.; Dahlhaus, R. Generalized Levinson–Durbin and burg algorithms. *Journal of Econometrics* **2004**, *118*, 129–149.

Preprints (www.preprints.org) | NOT PEER-REVIEWED | Posted: 6 February 2023 doi:10.20944/preprints202302.0092.v1

32. Beuter, A.; Glass, L.; Mackey, M.C.; Titcombe, M.S. *Nonlinear dynamics in physiology and medicine*; 2003.
33. Parreira, W.D.; Costa, M.H.; Bermudez, J.C. Stochastic behavior analysis of the Gaussian KLMS algorithm for a correlated input signal. *Signal Processing* **2018**, *152*, 286–291.
34. Dos Santos, V.A.; Parreira, W.D.; Fernandes, A.M.D.R.; Ovejero, R.G.; Leithardt, V.R.Q. Improving Speaker Recognition in Environmental Noise with Adaptive Filter. *IEEE Access* **2022**. doi:10.1109/ACCESS.2022.3225405.
35. Leite, M.; Parreira, W.D.; Fernandes, A.M.d.R.; Leithardt, V.R.Q. Image Segmentation for Human Skin Detection. *Applied Sciences* **2022**, *12*. doi:10.3390/app122312140.
36. de Freitas, M.P.; Piai, V.A.; Farias, R.H.; Fernandes, A.M.R.; de Moraes Rossetto, A.G.; Leithardt, V.R.Q. Artificial Intelligence of Things Applied to Assistive Technology: A Systematic Literature Review. *Sensors* **2022**, *22*. doi:10.3390/s22218531.
37. Parreira, W.D.; Bermudez, J.C.M.; Richard, C.; Tourneret, J.Y. Stochastic behavior analysis of the Gaussian kernel least-mean-square algorithm. *IEEE Transactions on Signal Processing* **2012**, *60*, 2208–2222.
38. dos SP Soares, A.; Parreira, W.D.; Souza, E.G.; de Almeida, S.J.; Diniz, C.M.; Nascimento, C.D.; Stigger, M.F. Energy-based voice activity detection algorithm using Gaussian and Cauchy kernels. 2018 IEEE 9th Latin American Symposium on Circuits & Systems (LASCAS). IEEE, 2018, pp. 1–4.
39. Soares, A.d.S.P.; Parreira, W.D.; Souza, E.G.; Nascimento, C.d.D.d.; Almeida, S.J.M.d. Voice Activity Detection Using Generalized Exponential Kernels for Time and Frequency Domains. *IEEE Transactions on Circuits and Systems I: Regular Papers* **2019**, *66*, 2116–2123. doi:10.1109/TCSI.2019.2895771.

Disclaimer/Publisher's Note: The statements, opinions and data contained in all publications are solely those of the individual author(s) and contributor(s) and not of MDPI and/or the editor(s). MDPI and/or the editor(s) disclaim responsibility for any injury to people or property resulting from any ideas, methods, instructions or products referred to in the content.